Chirality and Size Dependent Elastic Properties of Silicene Nanoribbons under Uniaxial Tension

Yuhang Jing[1,2,*], Yi Sun[1], Hongwei Niu[1], Jun Shen[2]

[1] Department of Astronautical Science and Mechanics, Harbin Institute of Technology, Harbin 150001, China
[2] School of Materials Science and Engineering, Harbin Institute of Technology, Harbin 150001, China
* Corresponding author: jingyh@hit.edu.cn

Abstract The mechanical properties of silicene are investigated using *ab initio* calculation and molecular dynamics simulations with different empirical potentials. The simulation results show that the calculated Young's modulus of bulk silicene with EDIP model is consistent with the *ab initio* calculations. The chirality has a significant effect on the critical strain and stress of bulk silicene under uniaxial tension. In addition, the Young's modulus depends strongly on the chirality and size of the silicene nanoribbon. The fracture process of a silicene nanoribbon is also studied.

Keywords Silicene, Young's modulus, Chirality and Size effects

1. Introduction

Graphene, which is a two-dimensional (2D) atomic layer of graphite, forms the basis of both 3D graphite and 1D carbon nanotubes. Since the discovery of graphene, graphene has attracted a worldwide attraction due to its extraordinary mechanical and electronic properties and potential applications [1-5]. The silicon analogue of graphene, the so called silicene, also attracts considerable scientific interest [6-8]. Recently, the possible growth of silicene nanoribbons on Ag (100), Ag (110), and Ag (111) substrates has been reported [9-11]. The electronic properties of silicene have also been investigated theoretically [12-14], some of which have been shown to be similar to those of graphene [12]. Thus, it can be expected that silicene can have the remarkable characters as graphene. Similar to graphene nanoribbons, the electronic properties of silicene nanoribbons are dependent of the structural size and chirality. Armchair silicene nanoribbons are semiconducting while the zigzag silicene nanoribbons are metallic when the width of the ribbons is broader [15]. However, compared with graphene, silicene have more potential applications in future nanoscale devices due to its compatibility with conventional Si-based electronic technology. Mechanical properties of nanoscale structures need to be understood in detail to enable design of high-performance and reliable micro/nanoelectromechanical systems (MEMS/NEMS) [16]. From a theoretical viewpoint, many correlative theoretical predictions have been performed in recent years and the attentions are mainly paid on the microstructural and electronic properties of the silicene [12-15]. The theoretical investigation of the mechanical properties of the silicene is also necessary and timely. However, the mechanical properties of silicene have not been reported so far. Therefore, in this work, *ab initio* calculations are performed to obtain robust predictions of the mechanical properties of the silicene, and then we investigate the chirality and size effects on the elastic properties of silicene nanoribbons using molecular dynamics (MD) simulations.

2. Simulation details

We employ *ab initio* calculations in order to obtain robust predictions of the mechanical properties of silicene using SIESTA code [17] and check different empirical potentials' accuracy. By means of extensive optimization, a user-defined double zeta plus polarization (DZP) basis set is constructed for the silicene. The Perdew-Burke-Ernzerhof (PBE) formulation of the generalized gradient approximation (GGA) for the exchange and correlation functional is used in the calculation to account for the electron-electron interactions. The k-grid sampling of 16×16×1 for the silicene, together with a meshcutoff of 200 Ry for the system are used in the calculation. Small stress is applied along zigzag or armchair direction of silicene and then relax the geometry until the forces on each atom are less than 0.01 eV $Å^{-1}$.

In order to study the chirality and size effects on the elastic properties of silicene nanoribbons, MD simulations are performed using LAMMPS [18]. Several inter-atomic potentials have been used in the MD simulations, including EDIP [19,20], Stillinger-Weber (SW) [21], Erhart-Albe [22], MEAM [23]. Isothermal-Isobaric (NPT) simulations are performed at a given temperature for 100 ps with a time step of 0.1 fs to let the system reach its equilibrium configuration. The strain is then applied along the uniaxial direction to perform uniaxial tensile tests. The applied strain rate is 0.005/ps. The pressure component vertical to the loading direction is controlled to maintain the uniaxial tensile condition. The strain increment is applied to the structure after every 10000 time steps with the step size of 0.1 fs. All the MD simulations are carried out at 300K and the temperature is controlled by employing the Nosé-Hoover thermostat [24]. The Velocity-Verlet algorithm is employed to integrate the equations of motion.

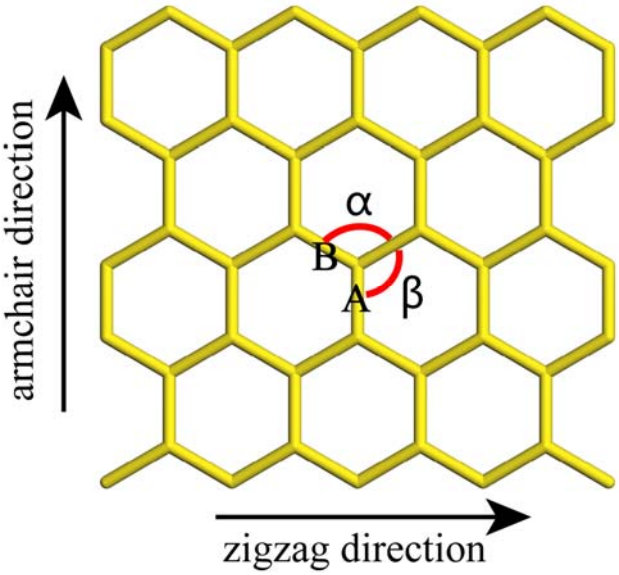

Figure 1 A silicene nanoribbon, along with the definitions of zigzag and armchair directions, bond types, and bond angles.

3. Results and discussion

As shown in Figure 1, we investigate the mechanical properties of rectangular bulk silicene in both the zigzag direction and armchair direction. The silicene thickness is assumed to 0.42 nm which is twice size of van der waals radius of silicon [25]. In *ab initio* calculations, the Young's modulus in both zigzag and armchair directions of bulk silicene with 60 atoms (1.94 nm × 2.01 nm) is calculated from $Y = \frac{1}{V_0}\frac{\partial^2 E}{\partial \varepsilon^2}$ with a low strain ($\leq 2\%$), where $\frac{\partial^2 E}{\partial \varepsilon^2}$ is the second derivative of the total energy with respect to the strain of the silicene and V_0 is the minimum total energy volume. The calculated results are 148.5 and 140.7 GPa along zigzag direction and armchair direction, respectively. In MD simulations, in order to investigate the effect of chirality on the mechanical properties of bulk silicene, we perform displacement-control uniaxial tensile tests in both zigzag and armchair directions of bulk silicene with 7168 atoms (around 21 nm × 21 nm) with periodic boundary conditions in the in-plane two directions. Figure 2 shows the strain-stress relations for uniaxial tensile tests in both zigzag and armchair directions from MD simulations. The Young's modulus is evaluated using the expression, $Y = \sigma / \varepsilon$ in the elastic region, where σ and ε are the stress and strain, respectively. Table I displays the Young's modulus of bulk silicene for different potentials, and a comparison with *ab initio* calculations is also shown. As we can see from Table I, the calculated Young's modulus of bulk silicene using EDIP model is a little bigger than the *ab initio* calculations because the EDIP model is a short ranged potential, which will lead to an increased stiffness [26]. The results from Erhart-Albe are a little smaller than the *ab initio* calculations. However, the stress increases dramatically when the strain reaches certain value (see

Figure 2). This awkward phenomenon results form the cut-off function in the Erhart-Albe (Tersoff-like) potential [27]. The results from SW and MEAM potentials are much lower than the *ab initio* calculations. Therefore, we select the EDIP model for the following calculations.

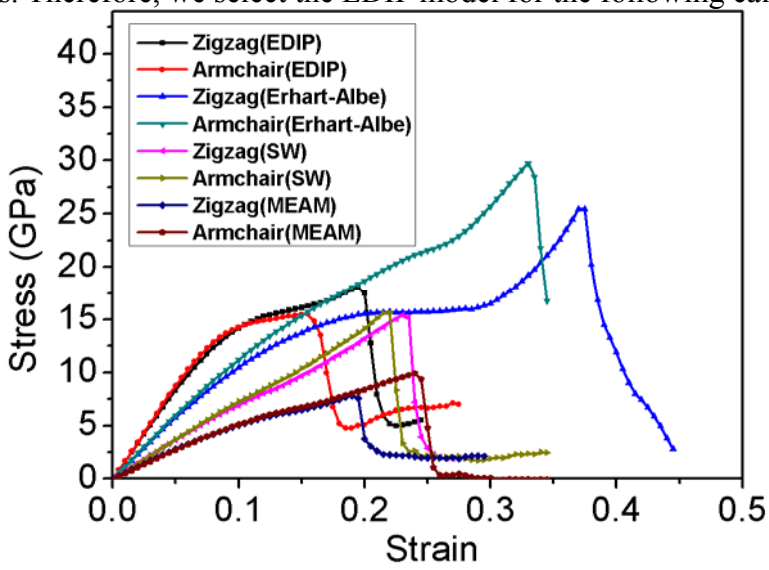

Figure 2 Strain-Stress relations of bulk silicene under tensile tests in the zigzag and armchair directions with different potential.

Table 1 Young's moduli for bulk silicene from *ab initio* calculations and different potential models. All values are in units of GPa.

Direction of tension	*Ab initio* results	EDIP	Erhart-ALbe	SW	MEAM
Zigzag direction	148.5	166.7	120.7	73.3	57.2
Armchair direction	140.7	170.8	121.2	67.0	56.1

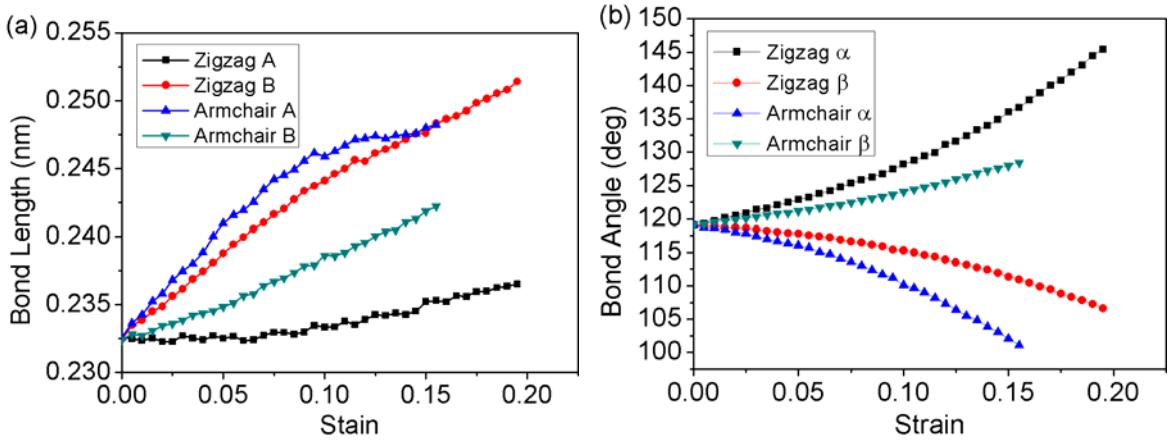

Figure 3 Evolutions of bond length (a) and bond angle (b) with a function of strain when uniaxial tension is applied on bulk silicene along zigzag and armchair directions.

As the strain increases, the chirality dependence becomes obvious for all potentials. As for EDIP model, the critical strain is 15.5% and 19.5% in the armchair and zigzag direction, respectively. The calculated critical stress of bulk silicene is 15.5 and 18.1 GPa in the armchair and zigzag direction, respectively. The critical strain and stress are different for zigzag and armchair load tests. To give more insight into this phenomenon, the variation of the bond length and bong angle with the strain in the tensile direction for zigzag and armchair cases are shown in Figure 3. One can see that in the zigzag loading case, the main bond elongation is experienced by bond B. In the armchair loading case, the main bond elongation is experienced by bond A. When the strain is smaller, the elongation ratio of amchair A is larger than that of zigzag B (see Figure 3(a)). However, the elongation ratio of amchair A become smaller and is lower than that of zigzag B when the strain is larger than 0.1. Moreover, the magnitude of the bond angle variation in the amchair direction tension test is larger

than that in the zigzag direction tension test when the strain is larger than 0.1. Smaller angle α can release stress which results in slower stress increase, which will enlarge the critical strain. Hence, the larger critical strain in zigzag direction tension than that in armchair direction tension can be understood.

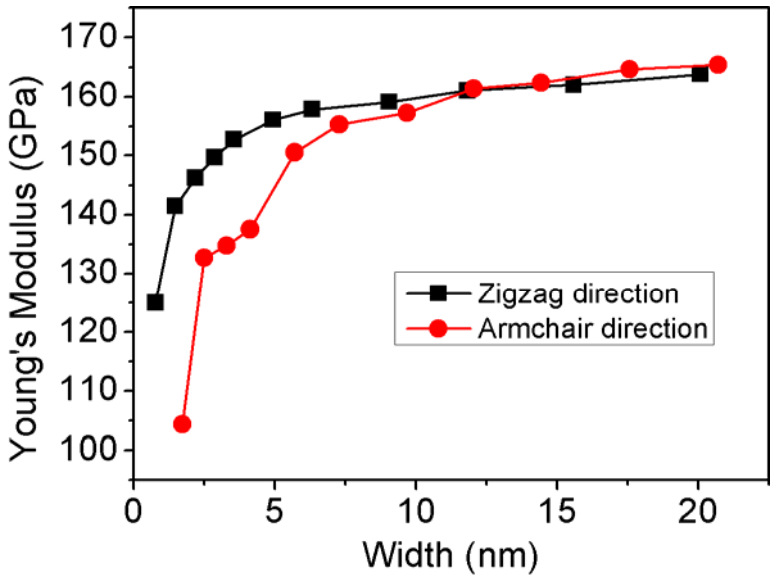

Figure 4 Young's modulus as a function of the silicene nanoribbon's width for uniaxial tension along the armchair and zigzag directions.

To study the size and chirality effects on the mechanical properties of silicene nanoribbons, deformation-control uniaxial tensile tests are performed. The width of square-shaped silicene nanoribbons in armchair and zigzag directions varies from 0.8 to 20.7 nm. An NVT ensemble is used with 10.0 nm vacuum space on each side of the nanoribbon. The Yong's modulus is calculated for armchair and zigzag directions using the above expression, $Y = \sigma / \varepsilon$ in the elastic region. In Figure 4 we plot the variation of Young's modulus as a function of the size of the silicene nanoribbon. It can be seen that Young's modulus along zigzag and armchair directions increases with the width of the nanoribbon. This variation is similar to the size-dependent Young's modulus of graphene nanoribbon [28]. For example, the size effect on Young's modulus is negligible when the width of the silicene nanoribbon is over 15.0 nm. Furthermore, significant chirality effects are found in the Figure 4. For the nanoribbons with the same size, Young's modulus is larger along the zigzag direction than along the armchair direction when the width of nanoribbon is smaller than 10.0 nm, which is consistent with the results for the graphene nanoribbon [28].

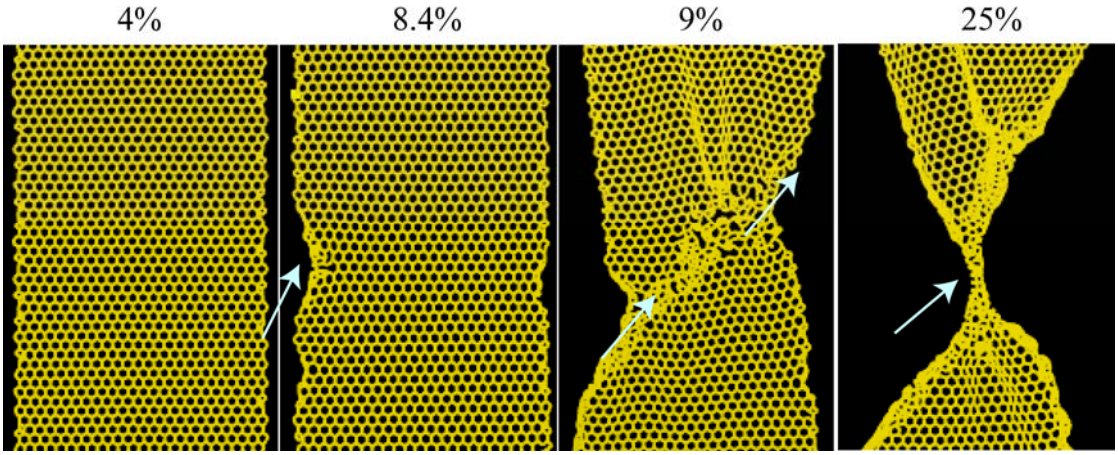

Figure 5 Snapshots of atomix configurations at various strains.

As shown in Figure 2, as the strain increase to certain value, the bulk silicene starts to fracture, which is same for silicene nanoribbon under uniaxial tension. Figure 5 presents the fracture process of an armchair silicene nanoribbon with the width of 9.7 nm. The applied strain rate is 0.0005/ps.

For small strains, both sides of nanoribbon shrink to release the deformation energy, and no structural defects appear at this stage. For larger strains, bond breakage in the edge is observed and spreads toward the center as the strain increases. With the strain increasing further more, we find that sliding happens, and many atoms rearrange in the neck region. The deformation mechanism of a shearing action is similar to that of silicon nanowire [29]. After the formation of the neck, the plastic deformations have been carried mainly through the reconstruction and rearrangement of the neck reion. Beyond this region, the nanoribbon keeps ordered structure and have no significant change. Despite that the EDIP model gives a considerably accurate Young's modulus of bulk silicene, a detailed analysis of the fracture behavior of silicene nanoribbons is still needed with different empirical potentials or *ab initio* calculations.

4. Conclusions

In this paper, the chirality and size effects on the mechanical properties of silicene nanoribbons are investigated based on atomistic simulation. Compared with the *ab initio* calculations, EDIP model of bulk silicene gives a more accurate Young's modulus than other empirical potentials. As for bulk silicene, uniaxial tensile test along the zigzag direction has a larger critical strain and stress compared to the armchair direction. The Young's modulus increases as the size of silicene nanoribbons increases. Significant slip activities are observed in MD simulations with EDIP model. Further theoretical and experimental studies are needed to study the mechanical properties of this new 2D silicon nanomaterial.

Acknowledgements

The work is supported by China Postdoctoral Science Foundation, and Fundamental Research Funds for the Central Universities under Grant No.HIT.NSRIF.2013031.

References

[1] C. Lee, X. Wei, J. W. Kysar, and J. Hone, Measurement of the Elastic Properties and Intrinsic Strength of Monolayer Graphene. Science 321 (2008) 385.
[2] C. A. Marianetti and H. G. Yevick, Failure Mechanisms of Graphene under Tension. Phys. Rev. Lett. 105 (2010) 245502.
[3] K. S. Novoselov, A. K. Geim, S. V. Morozov, et al., Thin Carbon Films. Science 306 (2004) 666.
[4] A. H. Castro Neto, F. Guinea, N. M. R. Peres, K. S. Novoselov, and A. K. Geim, The electronic properties of graphene. Reviews of Modern Physics 81 (2009) 109.
[5] C. Soldano, A. Mahmood, and E. Dujardin, Production, properties and potential of graphene. Carbon 48 (2010) 2127-2150.
[6] J. Kang, F. Wu, J. Li, Symmetry-dependent transport properties and magnetoresistance in zigzag silicene nanoribbons. Appl. Phys. Lett. 100 (2012) 233122.
[7] S. Lebegue, O. Topsakal, Electronic structure of two-dimensional crystals from *ab initio* theory. Phys. Rev. B 79 (2009) 115409.
[8] R. Qin, C. Wang, W. Zhu, Y. Zhang, First-principles calculations of mechanical and electronic properties of silicene under strain. AIP ADVANCES, 2 (2012) 022159.
[9] C. Leandri, H. Saifi, O. Guillermet, B. Aufray, Silicon thin films deposited on Ag(001): growth and temperature behavior. App. Surf. Sci. 177 (2001) 303.
[10] P. D. Padova, C. Quaresima, C. Ottaviani, et al., Evidence of graphene-like electronic signature in silicene nanoribbons. Appl. Phys. Lett. 96 (2010) 261905.
[11] C. Lin, R. Arafune, K. Kawahara, et al., Structure of Silicene Grown on Ag(111). Applied Physics Express 5 (2012) 045802.
[12] S. Cahangirov, M. Topsakal, E. Akturk, H. Sahin, S. Ciraci, Two- and One-Dimensional Honeycomb Structures of Silicon and Germanium. Phys. Rev. Lett. 102 (2009) 236804.
[13] Z. Ni, Q. Liu, K. Tang, et al., Tunable Bandgap in Silicene and Germanene. Nano lett. 12 (2012) 113.
[14] N. D. Drummond, V. Zolyomi, V. I. Fal'ko, Electrically tunable band gap in silicene. Phys. Rev. B 85 (2012) 075423.

[15] Y. Song, Y. Zhang, J. Zhang, D. Lu, Effects of the edge shape and the width on the structural and electronic properties of silicene nanoribbons. Appl. Surf. Sci. 256 (2010) 6313-6317.
[16] X. Li, B. Bhushan, K. Takashima, C. Baek, Y. Kim, Mechanical characterization of micro/nanoscale structures for MEMS/NEMS applications using nanoindentation techniques. Ultramicroscopy 97 (2003) 481-494.
[17] Soler JM, Artacho E, Gale JD, Garcia A, Junquera J, Ordejon P, et al. The SIESTA Method for *ab Initio* Order-N Materials Simulation. J Phys: Condens Matter 2002;14:2745-79.
[18] S. Plimpton. Fast Parallel Algorithms for Short-Range Molecular Dynamics. J. Comput. Phys. 117 (1995) 1.
[19] M.Z. Bazant, E. Kaxiras, J.F. Justo, Environment-dependent interatomic potential for bulk silicon. Phys. Rev. B 56 (1997) 8542.
[20] J.F. Justo, M.Z. Bazant, E. Kaxiras, V.V. Bulatov, S. Yip, Interatomic potential for silicon defects and disordered phases. Phys. Rev. B 58 (1998) 2539.
[21] F.H. Stillinger, T.A. Weber, Computer simulation of local order in condensed phases of silicon. Phys. Rev. B 31 (1985) 5262.
[22] P. Erhart and K. Albe, Analytical potential for atomistic simulations of silicon, carbon, and silicon carbide. Phys. Rev. B 71 (2005) 035211.
[23] M. I. Baskes. Modified embedded-atom potentials for cubic materials and impurities. Phys. Rev. B 46 (1992) 2727.
[24] W. G. Hoover, Canonical dynamics: Equilibrium phase-space distribututions. Phys. Rev. A 31 (1985) 1695-1697.
[25] A. Bondi, van der Waals Volumes and Radii. J. Phys. Chem., 68 (1964) 441-451.
[26] Y. Jing, Q. Meng, Molecular dynamics simulations of the mechanical properties of crystalline/amorphous silicon core/shell nanowires. Physica B 405 (2010) 2413-2417.
[27] O. A. Shenderova, D. W. Brenner, A. omeltchenko, X. Su, Atomistic modelling of the fracture of polycrystalline diamond. Phys. Rev. B 61 (2000) 3877-3888.
[28] H. Zhao, K. Min, N. R. Aluru, Size and Chirality Dependent Elastic Properties of Graphene Nanoribbons under Uniaxial Tension. Nano Lett. 9 (2009) 3012-3015.
[29] Y. Jing, Q. Meng, W. Zhao, Molecular dynamics simulations of the tensile and melting behaviours of silicon nanowires. Physica E 41 (2009) 685-689.